

# GROWTH OF NOVEL NONLINEAR OPTICAL CRYSTAL $\text{BaAlBO}_3\text{F}_2$ SUITABLE FOR HIGH POWER UV LIGHT GENERATION AND THEIR CHARACTERIZATION

N.Marimuthu and P.Sureshkumar\*

Material Research Center, Department of Physics, Velammal Engineering College, Chennai -600066, India

\*Corresponding author: sureshrath@yahoo.com

Received 24 August 2018 Received in revised form 28 August 2018 Accepted 30 August 2018  
Available Online 05 September 2018

## ABSTRACT

Barium aluminium borate difluoride ( $\text{BaAlBO}_3\text{F}_2$ -BABF) crystals have been grown by Middle seeded growth technique. Phase purity and crystallinity of grown crystals were investigated by powder X-ray diffraction study. The functional groups of the grown crystals were found by FTIR analysis. The UV and Photoluminescence study was performed to know the optical behavior of the crystal. The luminescence was found in a wide spectral region from 3.3-3.8eV which consists of narrow peaks due to different kinds of exciton annihilation and donor-acceptor pair recombination. The second harmonic generation output of  $\text{BaAlBO}_3\text{F}_2$  crystal was found to be 0.2 times lesser than potassium dihydrogen phosphate (KDP).

**Keywords:** NLO Crystals, Borate,  $\text{BaAlBO}_3\text{F}_2$ , Middle seeded growth, Flux growth

## 1. Introduction:

Nonlinear optical (NLO) borate crystals are often employed for high-power UV light generation because of their relatively high resistance to laser-CLBO),  $\text{KBe}_2\text{BO}_3\text{F}_2$  (KBBF),  $\text{Sr}_2\text{Be}_2\text{B}_2\text{O}_7$  (SBBO),  $\text{GdCa}_4\text{O}(\text{BO}_3)_3$  (GdCOB),  $\text{YCa}_4\text{O}(\text{BO}_3)_3$  (YCOB) and  $\text{Gd}_x\text{Y}_{1-x}\text{Ca}_4\text{O}(\text{BO}_3)_3$  (GdYCOB)[1-10] has been discovered. Barium aluminium borate difluoride,  $\text{BaAlBO}_3\text{F}_2$  (BABF) is an interesting and new nonlinear optical crystal belonging to the fluoroborate family. This crystal was first reported by Hu et al. in 2002[11]. This compound crystallizes in a hexagonal system with space group  $P6_3/m$ , with  $a=4.8879(6)$  Å and  $Z=2$ , non-centro symmetric structure and is an excellent candidate on UV light generation. Compared to other borate NLO crystals. BABF exhibits a number of advantages.. The BABF belongs to a noncentrosymmetric structure [12] and is an excellent candidate for UV light generation. BABF exhibits a number of advantages, such as more stable chemical-physical properties.

Generally borate crystals are relatively difficult to be grown to a large dimension with high optically homogeneity. The difficulty is attributed to the fact that flux compounds have higher viscosity and higher volatility in the high temperature solutions.

To overcome this proper choice of flux and flux/BABF ratio must be made. In the present work we have prepared single crystals of BABF and the grown crystals materials were subjected to XRD, FTIR, UV and Photoluminescence studies.

## II. Experiment- preparation of $\text{BaAlBO}_3\text{F}_2$

### i. Crystal growth

Starting materials which includes high purity  $\text{BaF}_2$  99.9%, Sigma-Aldrich), Diboron trioxide ( $\text{B}_2\text{O}_3$ , 99.8% Sigma-Aldrich), Aluminium oxide ( $\text{Al}_2\text{O}_3$ , 99.9% Merk), Lithium fluoride (LiF, 99.8% Sigma-Aldrich), Sodium fluoride (NaF, 99.8% Sigma-Aldrich) were taken in the molar ratio of  $\text{BaF}_2 : \text{B}_2\text{O}_3 : \text{Al}_2\text{O}_3 : \text{LiF} : \text{NaF} :: 2:3:1:5:2:0.6$  and total weight of 50g loaded in 75 ml Pt crucible. LiF,  $\text{B}_2\text{O}_3$  & NaF taken in the molar ratio 2:3:1:5:2:0.6 contribute to flux. The loaded crucible was then placed inside a pre-heated single zone furnace and melted. The crucible was kept at 1000°C for 12 h for homogenization. Use of pre-heated furnace avoids the formation of bubbles, more frothing and dissociation of materials.

### ii. Spontaneous nucleation technique

The experiments were carried out in a single zone vertical cylindrical furnace with SiC heating elements. The furnace was designed to ensure

uniform temperature in the heating zone. From many trials the crystallization process was optimized for the existing setup.  $\text{BaAlBO}_3\text{F}_2$  crystallization was observed in the temperature range of  $900^\circ\text{C}$  -  $750^\circ\text{C}$  with cooling rate of  $3^\circ\text{C/d}$ . Spontaneously nucleated tiny crystals were found to be floating on the surface of melt after 15 days. Small crystals of  $\text{BaAlBO}_3\text{F}_2$  were separated by mechanical fragmentation from the melt surface. It was observed that the crystals were mostly formed either on surface of melt or on crucible wall because of higher supersaturation at these points.

### iii. Middle seeded growth technique

The suitable molar ratio of raw and flux materials were fully charged in platinum crucible. It was placed in the electrical furnace and the temperature was raised to  $1000^\circ\text{C}$ . The solution was stirred by a platinum stirrer for 24 hr and then slowly cooled down below melting point. After the solution was homogenized for several hours, the seed was monitored and the solution temperature was adjusted until the saturation temperature was established. The growth was initiated by a decrease of the solution temperature. Then the seed was lowered about 10mm beneath of the solution surface. During the growth process, the cooling rate was set in the range of  $2^\circ\text{C/day}$ . The growing crystal was rotated at rotation speed between 20 and 30 rpm. When the growth process was completed after 15 days, the crystal was drawn slowly out of the solution surface, kept just above (10 mm) the solution and then cooled down to  $800^\circ\text{C}$  at the rate of  $10^\circ\text{C/h}$ . From this temperature the furnace was cooled at faster rate until it reaches room temperature. The ingot of solidified flux with crystals is shown in figure 1. The crystals harvested from the ingot is shown in figure 2.



Fig.1 Flux ingot



Fig.2  $\text{BaAlBO}_3\text{F}_2$  crystals

### III. Characterization

The X-ray powder patterns of these samples were recorded using Rigaku D/max-A X-ray diffractometer ( $\text{CuK}\alpha$ ,  $\lambda=1.54434 \text{ \AA}$ ) at the scanning rate of  $2^\circ/\text{min}$  and  $2\theta$  is varied from  $10$ – $70^\circ$ .

Fourier Transform Infrared spectroscopy was carried out at room temperature in the range of  $4000 - 450 \text{ cm}^{-1}$  using a Perkin Elmer Spectrum two FT-IR/ ATR Spectrometer. The powder form of each sample is placed in the sample holder and the FT-IR Spectrum is recorded by using ATR Diamond Accessory.

The optical absorption measurements were made using a Lambda 35 UV Winlab Spectrometer, in the range of  $190 - 1100 \text{ nm}$ . The photoluminescence (PL) spectrum and the PL decay time was recorded by JobinYvon spectrofluorometer (FLUOROLOG - FL3-11) with Xenon Lamp 450W as an excitation source in the range  $180$ – $1550 \text{ nm}$ . The NLO coefficient of grown  $\text{BaAlBO}_3\text{F}_2$  crystals was measured by using Kurtz-Perry powder method.

### IV. Result and discussion

#### i. X-Ray diffraction analysis $\text{BaAlBO}_3\text{F}_2$ crystal,

Powder X-ray diffraction studies were performed on the grown crystals to identify the phase formation and degree of crystal perfection. X-ray powder patterns of  $\text{BaAlBO}_3\text{F}_2$  were recorded using Bruker D4 X-ray diffractometer. Monochromatic intense X-ray of wavelength  $1.5418 \text{ \AA}$  ( $\text{CuK}\alpha$ ) was used. The sharp peaks are very well agreed with the diffraction peaks of  $\text{BaAlBO}_3\text{F}_2$  (ICDD: 01-071-2773).

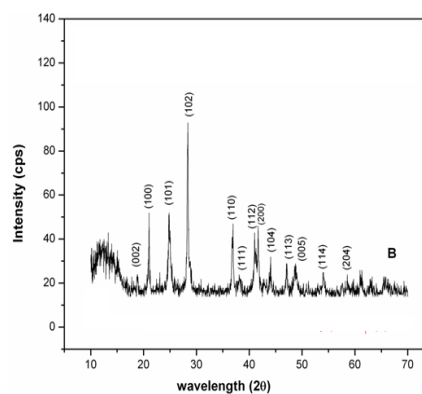


Fig.3 XRD of  $\text{BaAlBO}_3\text{F}_2$  crystal

## ii. Nonlinear optical studies for crystals

The as grown  $\text{BaAlBO}_3\text{F}_2$  crystals were subjected to second harmonic generation analysis by using Kurtz and Perry powder technique. The fundamental beam of 1064 nm from Q switched Nd: YAG laser was used to test the second harmonic generation (SHG) property of  $\text{BaAlBO}_3\text{F}_2$  crystal. Pulse energy 1.2 mJ/pulse and pulse width 8 ns with a repetition rate of 10Hz were used for the study. The SHG signal generated was confirmed from the emission of green light from the sample. The second harmonic generation output of  $\text{BaAlBO}_3\text{F}_2$  crystal was found to be 80mv and the SHG efficiency of  $\text{BaAlBO}_3\text{F}_2$  crystal was 0.2 times lesser than potassium dihydrogen phosphate (KDP).

## iv. FTIR spectra of the $\text{BaAlBO}_3\text{F}_2$ crystals

The FTIR spectra of  $\text{BaAlBO}_3\text{F}_2$  crystals in Fig.4 shows that the vibrational modes of the network present are mainly active in three infrared spectral regions as reported elsewhere. The band at  $516\text{cm}^{-1}$  is due to B-O-B vibrations of  $[\text{BO}_3]$  unit,  $585\text{cm}^{-1}$  is due to the bending and stretching vibrations of F-Al-F, whereas the band at  $695\text{cm}^{-1}$ ,  $712\text{cm}^{-1}$  and  $743\text{cm}^{-1}$  are due to the B-O-B vibrations of  $\text{BO}_3$  units. The bands at  $1276$ ,  $1395$  and  $1465\text{cm}^{-1}$  are due to the asymmetric stretching relaxation of the B-O bond of trigonal  $\text{BO}_3$  units. The band received at  $993\text{cm}^{-1}$  may be attributed to stretching vibrations of Al-O-B linkages.

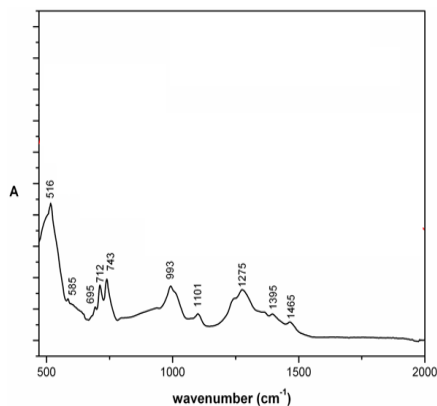


Fig.4 FTIR spectrum of  $\text{BaAlBO}_3\text{F}_2$  crystals

## v. UV-Visible spectroscopy

UV-visible reflectance spectra of  $\text{BaAlBO}_3\text{F}_2$  crystal show Fig.5. The absorption line for  $\text{BaAlBO}_3\text{F}_2$  crystal exhibited a band from 200 nm to 400 nm, which was due to the host absorption. There is no sharp absorption peaks received in the UV range.

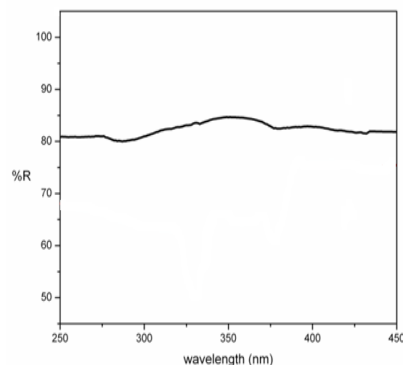


Fig.5 UV Visible spectrum of  $\text{BaAlBO}_3\text{F}_2$  crystal.

## vi. Photoluminescence of $\text{BaAlBO}_3\text{F}_2$ crystal

The photoluminescence (PL) spectra of  $\text{BaAlBO}_3\text{F}_2$  crystal are shown in Fig.6. It consists of a broad asymmetric band with a maximum at 350 nm ( $28571\text{cm}^{-1}$ ) under the excitation of 249 nm. PL spectra in Figure 6 is similar to photoluminescence spectra for KBBF family crystals excited at 249 nm at room temperature. It is dominated by a broad band in the 325-375 nm region with the peak position at 350 nm. Since this crystal sample is non-doped, we conclude that the reason for the luminescence must be from impurities or the crystal itself [13]. In their work on KBBF, RBBF and NBBF, transition metal ions and rare earth ions were found to be present in ICP-AES measurement. The result shows that Zn is detected in all the three samples in a ppm scale. The photoluminescence spectra of BABF family crystals were similar to that of the BZBF crystal which has Zn just with a difference in the intensities. Therefore, the luminescence may be caused by the Zn impurity in the crystals. Besides, the luminescence in a wide spectral region from 3.3-3.8 eV which consists of narrow peaks is due to different kinds of exciton annihilation and donor-acceptor pair recombination [14]. The main luminescence peak is observed at 3.5

eV which is associated with exciton bound to neutral donor. It is in good accordance with the observed peak at 369 nm in KBBF family crystals.

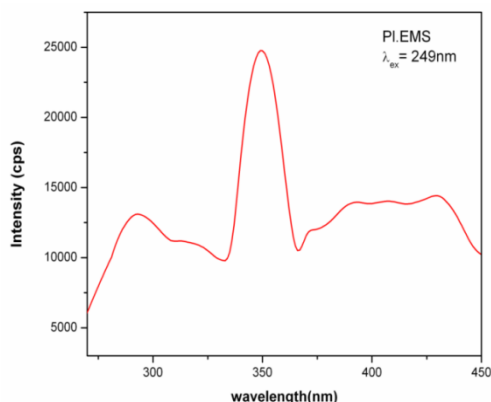


Fig.6. PL Emission spectrum of BaAlBO<sub>3</sub>F<sub>2</sub> glass ceramics

### V. Conclusion

Crystals of BaAlBO<sub>3</sub>F<sub>2</sub> have been grown by both spontaneous and middle seeded techniques. The crystalline phase of BaAlBO<sub>3</sub>F<sub>2</sub> crystal was confirmed by powder XRD analysis. The FTIR study shows that the functional groups present in the grown BaAlBO<sub>3</sub>F<sub>2</sub> crystal. The optical band gap was calculated by UV optical absorption studies. The PL excitation and emission spectra of BaAlBO<sub>3</sub>F<sub>2</sub> crystal were studied. The second harmonic generation output of BaAlBO<sub>3</sub>F<sub>2</sub> crystal was found to be 80mv and the SHG efficiency of BaAlBO<sub>3</sub>F<sub>2</sub> crystal was 0.2 times lesser than potassium dihydrogen phosphate (KDP). Based on these properties, the BaAlBO<sub>3</sub>F<sub>2</sub> crystal are considered as potential materials for UV generation.

### References

1. C. Chen, B. Wu, A. Jiang and G. You: Sci. Sin. B 28 (1985) 235.
2. C. Chen, Y. Wu, A. Jiang, B. Wu, G. You, R. Li and S. Lin: J. Opt. Soc. Am. B 6 (1989) 616.
3. Y. Wu, T. Sasaki, S. Nakai, A. Yokotani, H. Tang and C. Chen: Appl. Phys. Lett. 62 (1993) 2614.

4. T. Sasaki, I. Kuroda, S. Nakajima, K. Yamaguchi, S. Watanabe, Y. Mori and S. Nakai: Proc. Advanced Solid-State Lasers Conf. (1995) Vol. 24, p. 91.
5. Y. Mori, I. Kuroda, S. Nakajima, T. Sasaki and S. Nakai: Appl. Phys. Lett. 67 (1995) 1818.
6. L. Mei, Y. Wang, C. Chen and B. Wu: J. Appl. Phys. 74 (1993) 7014.
7. C. Chen, Y. Wang, B. Wu, W. Zeng and L. Yu: Nature 373 (1995) 322.
8. G. Aka, A. Kahn-Harari, D. Vivien, F. Salin, J. Godard and J. M. Benitez: Eur. J. Solid State Inorg. Chem. 33 (1996) 727.
9. T. Iwai, M. Kobayashi, H. Furuya, Y. Mori and T. Sasaki: Jpn. J. Appl. Phys. 36 (1997) 236.
10. H. Furuya, M. Yoshimura, T. Kobayashi, K. Murase, Y. Mori and T. Sasaki: J. Cryst. Growth 198/199 (1999) 560
11. Zhang-Gui HU, Masashi YOSHIMURA, Kenichi MURAMATSU, Yusuke MORI and Takatomo SASAKI, Jpn. J. Appl. Phys. Vol. 41 (2002) pp. L 1131–L 1133
12. H. Park and J. Barbier: J. Solid State Chem. 155 (2000) 354.
13. Lijuan Liu, Qian Huang, Mingjun Xia, Shu Guo, Xiaoyang Wang, Chuangtian Chen, doi.org/10.1016/j.jcrysgro.2016.10.058
14. Larisa Grigorjeva, Donats Millers, Journal of Physics: Conference series 93 (2007), 012036, 1-8.